ACS APPLIED MATERIALS & INTERFACES

www.acsami.org

Research Article

Photoimageable Organic Coating Bearing Cyclic Dithiocarbonate for a Multifunctional Surface

Sol An, Jieun Nam, Catherine Kanimozhi, Youngjoo Song, Seungjun Kim, Naechul Shin, Padma Gopalan,* and Myungwoong Kim*

Cite This: *ACS Appl. Mater. Interfaces* 2022, 14, 3274−3283

Read Online

ACCESS | Metrics & More | Article Recommendations | Supporting Information

ABSTRACT: We report the fabrication of photocross-linkable and surface-functionalizable polymeric thin films using reactive cyclic dithiocarbonate (DTC)-containing copolymers. The chemical functionalities of these material surfaces were precisely defined with light illumination. The DTC copolymers, namely, poly(dithiocarbonate methylene methacrylate−*random*-alkyl methacrylate)s, were synthesized via reversible addition−fragmentation chain transfer polymerization, and the reaction kinetics was thoroughly analyzed. The copolymers were cross-linked into a coating using a bifunctional urethane cross-linker that contains a photolabile *o*-nitrobenzyl group and releases aniline upon exposure to light. The nucleophilic attack of the aromatic amine opens the DTC group, forming a carbamothioate bond and generating a reactive thiol group in the process. The surface concentrations of the unreacted DTC and thiol were effectively controlled by varying the amounts of the copolymer and the cross-linker. The use of methacrylate comonomers led to additional reactive surface functionality such as carboxylic acid via acid hydrolysis. The successful transformations of the resulting DTC, thiol, and carboxylic acid groups to different functionalities via sequential nucleophilic ring opening, thiol−ene, and carbodiimide coupling reactions under ambient conditions were confirmed quantitatively using X-ray photoelectron spectroscopy. The presented chemistries were readily adapted to the immobilization of complex molecules such as a fluorophore and a protein in lithographically defined regions, highlighting their potential in creating organic coatings that can have multiple functional groups under ambient conditions.

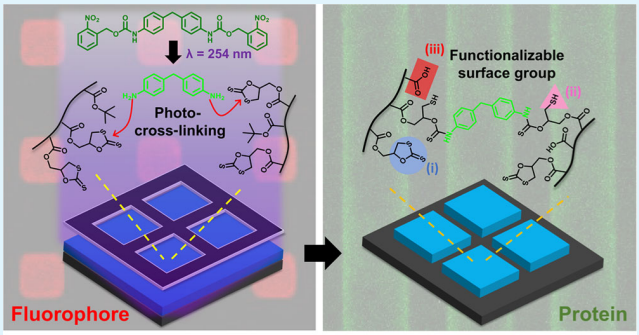

KEYWORDS: *multifunctional surface, cross-linkable copolymer, photoactivated cross-linker, surface modification, photopatternable polymer thin film, post-patterning modification*

INTRODUCTION

Imparting a desired function to the surface is crucial for attaining specific surface properties for targeted applications. One of the effective strategies is the deposition of a stable organic thin film on the surface, which can preset the desired functionalities. These functionalities can also be dynamically altered via chemical transformations, thus expanding their potential range of applications. The fine-tuning of surface wettability is a good example of such a strategy, as it allows the control of the self-assembly behavior of thin films comprising overlying block copolymer.[1,2] Other design strategies include the modification of the dielectric surface (which can improve the performance of organic thin-film transistors),[3−5] the grafting of hydrophilic zwitterionic polymer brushes (which is used for the formation of antifouling or antibacterial surfaces),[6−8] and the immobilization of oligopeptides with specific sequences onto the surface of the polymeric layer (which is used for the enhancement of cell adhesion).[9,10]

A wide array of strategies have been used for the surface engineering with organic thin films that include the deposition of a polymer solution onto the target surface by spraying, dipping, or spin-coating.[11−15] Other fabrication techniques are post-deposition processes, including the illumination of the layer with high-energy light such as X-ray and UV light,[16,17] and treatment with plasma.[18] These strategies are also commonly used to tune the properties of coatings, such as surface wettability.[16,19] The post-deposition processes can also lead to the incorporation of initiators for atom transfer radical polymerization, which can be used for the growth of a polymer brush to form a highly stable layer.[20]

Among the available surface modification methods, the cross-linking of a deposited organic thin film upon heat treatment or light illumination has been utilized for the rapid

Received: October 11, 2021
Accepted: December 22, 2021
Published: January 4, 2022

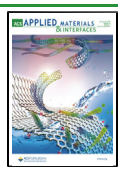

Scheme 1. Mechanism and Process to Fabricate Photocross-Linked Patterns in the Bicomponent Thin Film

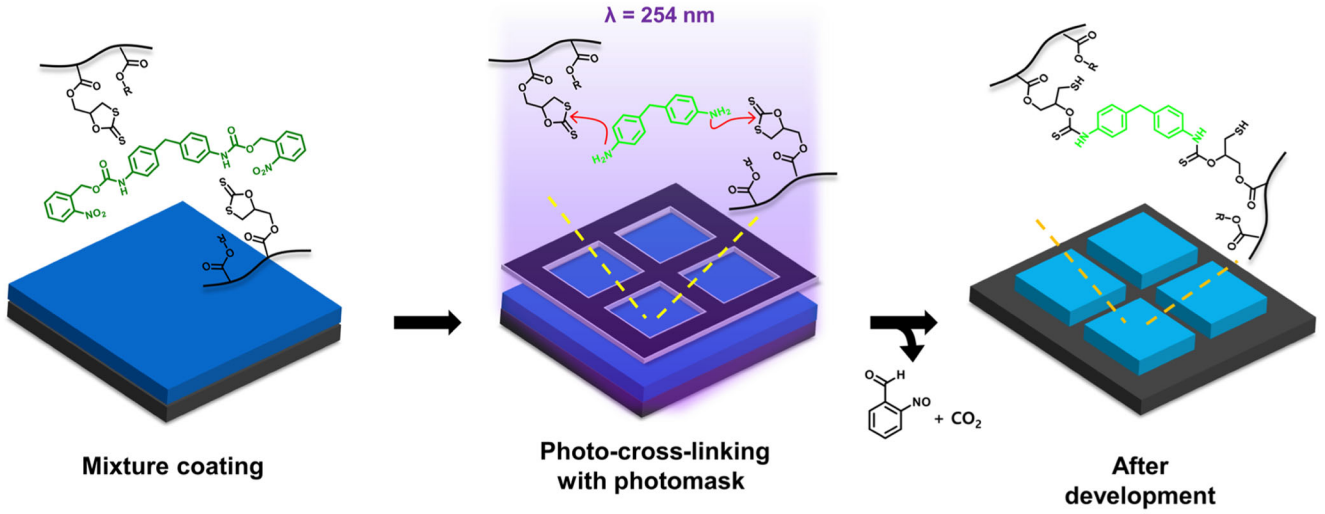

Scheme 2. RAFT Copolymerization of DTCMMA with Different Methacrylate Comonomers

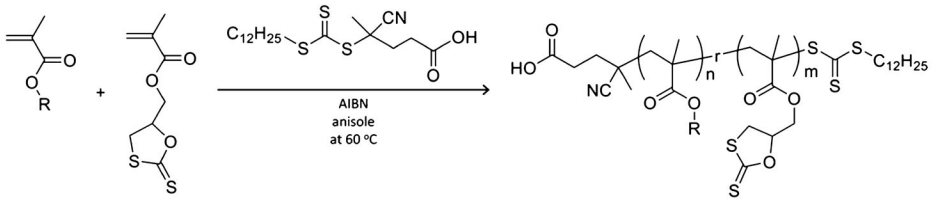

and efficient fabrication of highly stable thin films.[21,22] With this type of stable coating, the direct grafting of functional molecules and polymers onto the surface by chemical bonding with highly efficient chemical reactions has also been shown to be a practical approach to surface engineering.[13,23−29] In particular, the post-cross-linking modification of organic surfaces with specific chemical reactions defines new multiple chemical functionalities that can modify the physical and chemical properties of thin films without any complications due to the possible incompatibility of several polymeric components with different chemical functionalities. Other examples include the control of the behaviors of living tissues at the cellular level with the sequentially modified cross-linked polymer thin films to immobilize oligopeptides with specific sequences. With this type of coating, the fabrication of the chemical patterns makes the applicability of thin films further versatile toward a multifunctional surface, for example, the control of dynamic behaviors of specific cells.[30,31]

Ideal design guidelines of the surface coating include (i) high stability to subsequent modifications, (ii) a set of orthogonal functionalities that can allow simultaneous reaction without any cross-talk, and (iii) possession of functional groups in a spatially selective and quantifiable manner. Herein, we demonstrate the design and realization of a bicomponent photocross-linkable system comprising of a random copolymer of cyclic dithiocarbonate methylene methacrylate (DTCMMA) and alkyl methacrylates (methyl methacrylate (MMA), ethyl methacrylate (EMA), *n*-butyl methacrylate (*n*BMA), and *t*-butyl methacrylate (*t*BMA)) achieved by reversible addition−fragmentation chain transfer (RAFT) polymerization and a bifunctional cross-linker having two *o*-nitrobenzyl urethane groups. The cross-linker is deprotected to amines upon UV light illumination (Scheme 1),[32] which readily reacts with cyclic dithiocarbonate (DTC) pendant groups of the copolymer to cross-link the film. By controlling the amount of the cross-linker, the concentration of the residual unreacted DTC ring can be modulated for subsequent functionalization. We further show that three distinct functional groups can be added to this cross-linked coating through a cascade of reactions. First, the residual DTC rings can be leveraged for further post-cross-linking modification with primary amines, which has been known. Second, the DTC ring-opening reaction results in the release of a thiol group that can react with alkenes via thiol−ene click reaction. Third, a specific form of the alkyl methacrylate comonomer provides a further reactive group, such as carboxylic acid, that can be transformed to a third functionality on the surface via carbodiimide coupling reaction with a primary amine compound. The photopatternable thin film platform was readily applied to incorporate structurally complex functional molecules and biological polymer in lithographically defined regions, highlighting the potential of these coatings for interfacial modification in general and in the field of biotechnology. The synthetic and analytical methodologies described here offer a versatile means for creating a layer which can be used to produce reactive and functional surfaces and patterns with a high degree of complexity through simple, efficient, readily scalable, and quantitative approaches.

MATERIALS AND METHODS

Materials. Unless otherwise stated, all reagents were used as received. MMA (Daejung Chemicals, >99%), EMA (TCI Chemicals, >98%), *n*BMA (Alfa Aesar, 99%), and *t*BMA (TCI Chemicals, >98%) were passed through a neutral aluminum oxide column to remove the

https://doi.org/10.1021/acsami.1c19559
ACS Appl. Mater. Interfaces 2022, 14, 3274−3283

inhibitor before polymerization. 2,2′-Azobis(2-methylpropionitrile) (AIBN) was purchased from Junsei Chemicals and recrystallized from methanol before use. Glycidyl methacrylate (97%), 4-cyano-4-[(dodecylsulfanylthiocarbonyl)sulfanyl]pentanoic acid (CDTPA; 97%), carbon disulfide (CS_2; ≥99%), 4,4′-methylenebis(phenyl isocyanate) (98%), 2,2-dimethoxy-2-phenylacetophenone (DMPA; 99%), allyl bromide (AB; 99%), bovine serum albumin (BSA; 95%), fluorescein isothiocyanate isomer I (FITC; >90%), and aqueous ammonium thioglycolate solution (60% in H_2O) were obtained from Sigma-Aldrich Co. Ltd. 2-Nitrobenzyl alcohol (97%) and 4-fluorobenzyl amine (FA; >98%) were purchased from Alfa Aesar. Dithiothreitol (DTT, 0.1 M), tetramethylrhodamine (TAMRA) amine (5-isomer), and phosphate-buffered saline (PBS; 10× solution, pH 7.4 ± 0.1) were supplied by Thermo Scientific, Lumiprobe, and Fisher Bioreagents, respectively. All other chemicals were purchased from TCI Chemicals. DTCMMA was synthesized using a previously reported procedure.[33,34]

General Copolymerization. The copolymerization of DTCMMA with four methacrylates (MMA, EMA, *n*BMA, or *t*BMA) was conducted by RAFT polymerization (Scheme 2). Typically, a selected monomer (13.00 mmol), DTCMMA (5.50 mmol), AIBN (0.027 mmol), CDTPA (0.05 mmol), and anisole (2.5 g) were added into a Schlenk flask with a magnetic stirring bar, followed by degassing with three freeze−pump−thaw cycles. Copolymerization was carried out in an oil bath at 60 °C. Upon copolymerization for a desired time, the mixture was cooled to room temperature and quenched by exposure to air. A small amount of the resulting solution was taken to measure the conversion, while the remaining solution was added to methanol for precipitation. The resulting yellow solid was collected by vacuum filtration, followed by drying in a vacuum oven.

Synthesis of the Photocross-Linker. A mixture of 4,4′-methylenebis(phenyl isocyanate) (8 mmol), 2-nitrobenzyl alcohol (16 mmol), and dibutyltin dilaurate (0.15 mmol) was mixed in 30 mL of tetrahydrofuran (THF). The reaction proceeded at room temperature for 14 h. The solution was then concentrated by a rotary evaporator, followed by recrystallization in hexane. The product was collected by vacuum filtration, followed by drying in a vacuum oven overnight. ^{1}H NMR (400 MHz, DMSO-d_6): δ 9.96−9.65 (2H), 8.20−8.04 (2H), 7.86−7.73 (2H), 7.73−7.64 (2H), 7.64−7.53 (2H), 7.45−7.20 (4H), 7.20−6.96 (4H), 5.55−5.36 (4H), 3.89−3.67 (2H).

Photocross-Linking of the Thin Films. Either the synthesized poly(DTCMMA-*r*-*n*BMA) or poly(DTCMMA-*r*-*t*BMA) was dissolved with the photocross-linker in cyclopentanone. The typical concentration of the copolymer was 2.5 wt %, and the amount of photocross-linker was varied from 0.10 to 0.50 in mole ratio of photocross-linker compared to DTC unit in the copolymer. The silicon wafers were washed with acetone, isopropyl alcohol, and toluene and dried with a stream of nitrogen. The formulated solutions were spin-coated onto the silicon wafers. The spin-coated samples were then exposed to UV light (λ = 254 nm) for a desired time. After annealing at room temperature for 30 min, the samples were immersed in cyclopentanone for 5 min and then immersed again in fresh cyclopentanone for 5 min. The resulting samples were dried under a stream of nitrogen. For the photopatterning process, a photomask (18 μm line/18 μm space, 15 μm × 15 μm square with 25 μm space) was placed on the thin film sample, followed by exposure to an optimized intensity of UV light. The exposed samples were developed by immersion in cyclopentanone for 5 min, followed by additional immersion in fresh cyclopentanone for 5 min.

Post-cross-linking Surface Functionalization Reactions. Cross-linked thin films from poly(DTCMMA-*r*-*n*BMA) and poly(DTCMMA-*r*-*t*BMA) were subjected to surface reactions. In the first reaction, FA was dissolved in THF to a concentration of 10 wt %. Then, the thin film was immersed in 1 g of FA solution at room temperature for 30 min. After the reaction, the thin film was washed with cyclopentanone. In the second reaction, 10 wt % AB (1.0 g) was dissolved in THF, and 0.1 g of DMPA was added. The resulting thin-film sample was dipped in the solution, followed by UV light (365 nm) illumination for 1 h. Some samples were treated with DTT solution in THF (10 mM) before the reaction. After the reaction, the film was washed with cyclopentanone. For poly(DTCMMA-*r*-*t*BMA), the film could release further functional group, that is, carboxylic acid, by the deprotection of the *t*-butyl group. The film was immersed in a 10 wt % trifluoroacetic acid solution in dichloromethane (DCM), followed by washing with cyclopentanone. An 1-ethyl-3-(3-dimethylaminopropyl)carbodiimide hydrochloride (EDC) coupling reaction was then carried out by immersing the sample in a mixed solution of 0.30 g of 4-iodobenzyl amine (IA), 0.40 g of EDC, 0.24 g of *N*-hydroxysuccinimide, and 12 mL of DCM. After reacting for 8 h, the thin film was washed with cyclopentanone. For immobilization of a fluorescent molecule, the photocross-linked thin film was immersed in a toluene solution of TAMRA amine (0.15 wt %) and shaken gently for an hour at room temperature. The sample was then washed with copious amounts of toluene. For grafting BSA, the photocross-linked thin film was immersed in a 0.5 mg/mL PBS solution of BSA, followed by gentle shaking for 1 h at room temperature. The sample was washed with an excess of deionized (DI) water. BSA was labeled with FITC by immersing the thin film in a FITC solution (5.0 mg in a mixed solution of 0.2 mL of DMSO and 10 mL of PBS) for 1 h in the dark. The sample was then washed with DI water.

Functionalization of Poly(DTCMMA-*r*-*t*BMA) in Solution. 2.00 g of poly(DTCMMA-*r*-*t*BMA) (M_n = 3.72 kg/mol, $Đ$ = 2.60) was dissolved in 8.49 g of THF. FA (0.55 g, 4.36 mmol) was then added to the polymer solution. The mixture was stirred at room temperature for 30 min. The resulting solution was precipitated in methanol, and a yellow powder was collected by vacuum filtration. (M_n^{NMR} = 4.57 kg/mol, yield = 53%) For the reaction of the released thiol group and AB, 0.22 g of poly(DTCMMA-*r*-*t*BMA) (reacted with FA) was fully dissolved in 7.10 g of THF. AB (0.79 g, 6.52 mmol) was then added to the solution. A certain amount of DMPA was added to adjust its molar ratio to the AB or the thiol. The mixture was stirred at room temperature for 1 h under illumination with a 365 nm light. Yellow solids were obtained by precipitation in methanol and were collected by vacuum filtration (yield = 43%).

Characterization. A Thermo Scientific UltiMate 3000 chromatography system was used for size exclusion chromatography (SEC). THF was used as the eluent at a flow rate of 1 mL/min at 35 °C. Molecular weight information was obtained by analyzing the chromatograms with the calibration curve from the standard polystyrene samples (1.2−2700 kg/mol). ^{1}H and ^{13}C NMR spectra were obtained using a JEOL JNM-ECZ400S 400 MHz spectrometer in $CDCl_3$ or DMSO-d_6. The thicknesses of the fabricated thin films were measured using a spectroscopic ellipsometer (SE MG-1000, Nano-View Co. Ltd.; 350 nm < λ < 840 nm). The chemical structures and compositions of the thin films were studied by X-ray photoelectron spectroscopy (XPS) using a Thermo Scientific K-Alpha. Confocal laser scanning microscopy (CLSM; LSM 510 META) was used to detect the FITC ($\lambda_{excitation}$ = 488 nm) and TAMRA ($\lambda_{excitation}$ = 543 nm) present on the thin films and micropatterns. A high-resolution mass spectrum was acquired on a JMS900 mass spectrometer with the fast atom bombardment method at the Korea Basic Science Institute (Daegu, Korea).

RESULTS AND DISCUSSION

Copolymerization of DTCMMA with Alkyl Methacrylates. We first performed the homopolymerization of DTCMMA via free-radical polymerization; the homopolymers with a modest molecular weight showed extremely poor solubility in common solvents such as THF, DCM, anisole, toluene, ethyl acetate, and cyclopentanone. The solubility issue can be addressed by introducing a comonomer, as it was reported that a copolymer of DTCMMA and *n*BMA, namely, poly(DTCMMA-*r*-*n*BMA), synthesized by free-radical polymerization, was soluble in common solvents, though dispersity was not well controlled ($Đ$ > 2.7 at a f_{DTCMMA} of 0.3).[35] To access soluble copolymers of DTCMMA with narrow

https://doi.org/10.1021/acsami.1c19559
ACS Appl. Mater. Interfaces 2022, 14, 3274−3283

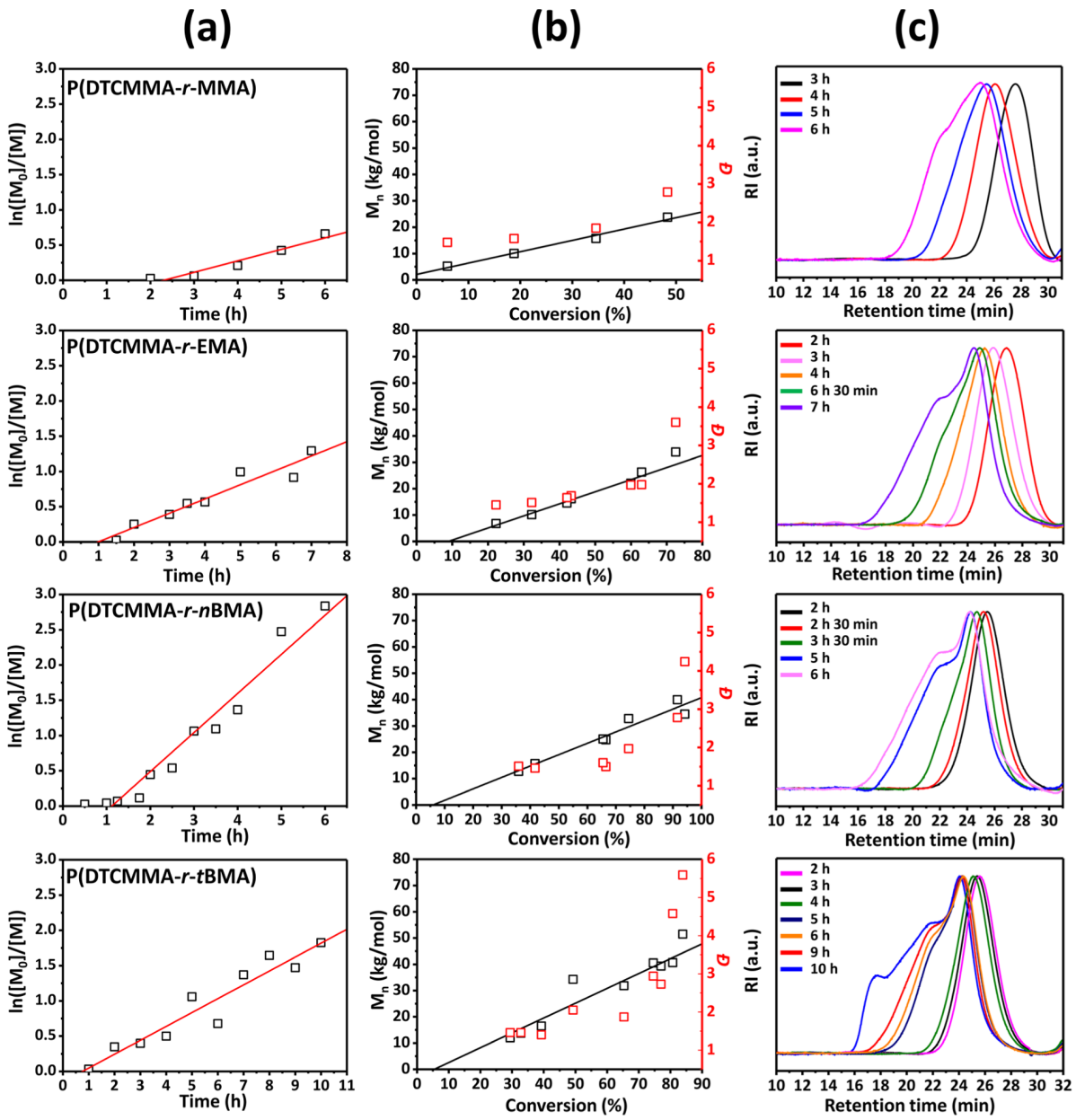

Figure 1. (a) Kinetic plots of copolymerization and (b) number-average molecular weight (M_n, left *y*-axis) and dispersity ($Đ$, right *y*-axis) as a function of polymerization conversion. (c) SEC chromatograms as a function of polymerization time.

molecular weight distribution, we conducted the RAFT copolymerization of DTCMMA and *n*BMA in anisole. The feed ratio of DTCMMA (f_{DTCMMA}) was varied from 0.10 to 0.90. The copolymers prepared with a f_{DTCMMA} of ≤0.30 were soluble in polar solvents such as THF, DMSO, and cyclopentanone, which make evaluation of composition and molecular weight by ^{1}H NMR and SEC analyses feasible.

We further systematically investigated RAFT copolymerizations of DTCMMA with MMA, EMA, *t*BMA, and *n*BMA with a f_{DTCMMA} of 0.30 (Scheme 2). Typically, the propagation kinetics of the RAFT polymerization follows the pseudo-first-order kinetic equation of $\ln([M]_0/[M]) = k_p^{app}t$, where [M] and $[M]_0$ are the monomer concentration at time t and the initial monomer concentration, respectively, and k_p^{app} is the apparent propagation rate constant. Figure 1a shows the kinetic plots of copolymerization with the four methacrylates. The kinetics of all four copolymerizations followed a pseudo-first-order reaction. Hence, the concentration of the activated chain end is in a steady state over the copolymerization. The observed k_p^{app} and induction periods (t_{id}) of the four copolymerizations are determined from the kinetic plots and are summarized in Table 1. Figure 1b shows the plots of the average molecular weight (M_n) and dispersity ($Đ$) of the

Table 1. Obtained Apparent Propagation Rate Constants and Induction Periods of the Copolymerization of DTCMMA with Different Comonomers

comonomer	k_p^{app} (h^{-1})	t_{id} (h)
MMA	0.16 ± 0.02	2.31
EMA	0.20 ± 0.02	1.00
*n*BMA	0.55 ± 0.04	1.12
*t*BMA	0.20 ± 0.02	0.76

https://doi.org/10.1021/acsami.1c19559
ACS Appl. Mater. Interfaces 2022, 14, 3274−3283

Scheme 3. Synthesis of a Photocross-Linker

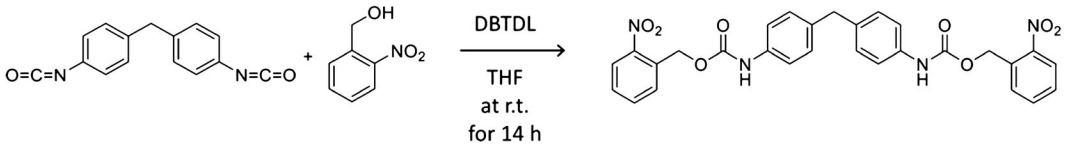

synthesized copolymers as a function of conversion. M_n increases linearly with conversion for all copolymerizations, which is typically observed kinetics for reversible deactivation radical polymerizations, including RAFT polymerization.[36] Interestingly, $Đ$ rapidly increases to values above 2 when the conversion is higher than 0.5. The shape of the SEC traces of the four copolymers with increased conversion (Figure 1c) changes from unimodal to multimodal when $Đ$ exceeds 3, which is in agreement with the results of previous reports on the free-radical copolymerization of DTCMMA with *n*BMA.[35] These results imply that, at higher conversion, certain but inconsiderable side reactions, such as chain transfer[37] or ring-opening, and the coupling reaction of the polymer chains into a disulfide bond, contribute to the increasing dispersity.[38,39] Despite the increase of the $Đ$, the monomer was consumed with following the linear trend in Figure 1b, implying that the side reactions do not significantly affect the radical-based propagation process based on the RAFT polymerization mechanism. Based on the kinetic studies, poly(DTCMMA-*r*-*n*BMA) and poly(DTCMMA-*r*-*t*BMA) ($0.24 < F_{DTCMMA} < 0.33$; determined with ^{1}H NMR) were obtained at moderate conversion to ensure well-preserved DTC rings that can be further functionalized after thin film fabrication processes (Figures S1–S3, Tables S1 and S2). The deviation of actual copolymer compositions from the feed composition suggests that the reactivity of the activated DTCMMA at the growing chain end is likely different from that of the methacrylate comonomers. The poor solubility limited the further estimation of the actual composition of the DTCMMA copolymers at a f_{DTCMMA} of >0.3, which impedes the further study of the reactivity ratio.

Photocross-Linked DTC Copolymer Thin Films. The pendant cyclic DTC can react efficiently with a primary amine, even at room temperature, and the ring-opening reaction results in the selective formation of thiol instead of alcohol.[33] To exploit this reaction to photocross-link the DTC-containing copolymer, a cross-linker that can provide multiple primary amine groups upon light illumination is required (Scheme 1). This was achieved with a bis(2-nitrobenzyl)methylenebis(1,4-phenylene)dicarbamate cross-linker by reacting a diisocyanate compound with *o*-nitrobenzyl alcohol (Scheme 3; Figures S4–S6).[40] The nitrobenzyl group can be cleaved upon UV light illumination to release two *p*-aniline groups,[41] which can open the DTC ring of the copolymer and leads to photocross-linking (Scheme 1). The many advantages of this design are its ease of synthesis, high stability under dark and ambient conditions, and facile deprotection at room temperature without the use of any photoinitiator or additives.

We prepared solutions containing the photocross-linker and copolymers with DTC unit/cross-linker molar ratios varying from 1:0.1 to 1:0.5 (Table S2). The thin films were fabricated by spin-coating onto silicon substrates. The cross-linking efficiencies of poly(DTCMMA-*r*-*n*BMA) and poly(DTCMMA-*r*-*t*BMA) (DTC unit/cross-linker = 1:0.5) as a function of exposure dose (Figure S7) were higher than 0.80 at 500 mJ/cm^2. The absence of any post-exposure treatments highlights the effective cross-linking reaction under mild conditions. Furthermore, the network was successfully formed with a relatively small amount of the cross-linker regardless of the type of the comonomer, suggesting that the amount of unreacted DTC ring on the surface is maximized by changing the composition of the system.

The resulting films were investigated through XPS studies to determine their chemical compositions (Figures 2 and S8, Table S3). The multiplex spectrum of the N 1s region before UV illumination showed a large peak at ≈399.8 eV assigned to the N atom from the urethane group in the cross-linker and a peak at ≈406 eV assigned to the N atom in the NO_2 group. After UV exposure, the peak at ≈406 eV notably decreased, indicating the successful deprotection of the *o*-nitrobenzyl group in the cross-linker. In our system, the deprotection of one cross-linker leads to the release of two primary amine groups that will react with two DTC units. Because two DTC units have four sulfur atoms and the activated cross-linker molecule has two nitrogen atoms, the stoichiometric reaction of all amines and DTCs present in the material will lead to a N/S atomic percent ratio of 0.5. Hence, the quantitative analysis of N %/S % through XPS measurements was used to evaluate the yield of the cross-linking reaction. The N %/S % for poly(DTCMMA-*r*-*n*BMA) and poly(DTCMMA-*r*-*t*BMA) with a DTC unit/cross-linker molar ratio of 1:0.5 was 0.314

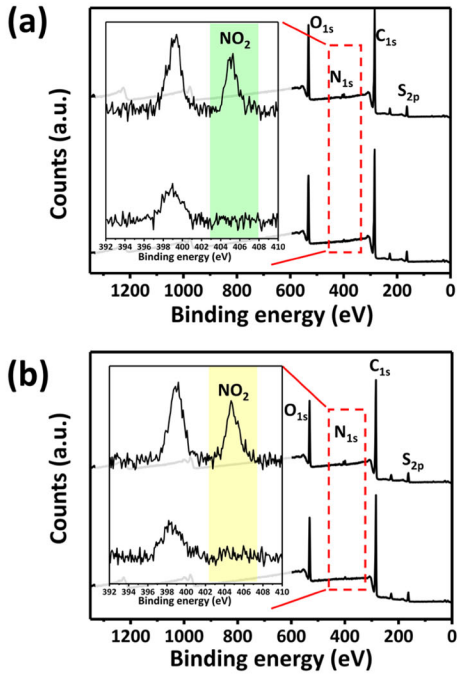

Figure 2. Representative XPS survey spectra before (top) and after (bottom) UV light illumination of (a) poly(DTCMMA-*r*-*n*BMA) thin films (DTC unit/cross-linker = 1:0.5) and (b) poly(DTCMMA-*r*-*t*BMA) thin films (DTC unit/cross-linker = 1:0.5).

https://doi.org/10.1021/acsami.1c19559
ACS Appl. Mater. Interfaces 2022, 14, 3274–3283

Scheme 4. Surface Modification via Subsequent Multiple Reactions to Obtain a Stable Organic Thin Film with High Complexity of Chemical Functionality[a]

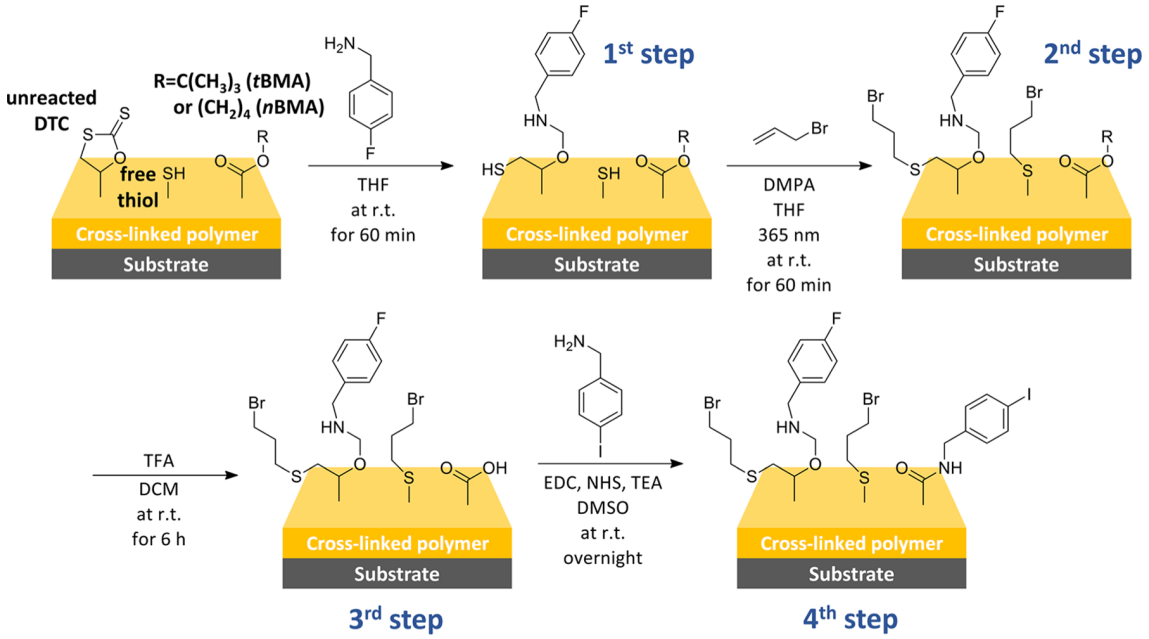

[a]The 3rd and 4th steps are for the thin film fabricated with poly(DTCMMA-*r*-*t*BMA) (R: *t*-butyl group).

and 0.516, respectively, which translates to reaction yields of 0.63 and quantitative conversion. These results suggest that a certain amount of DTC units remains intact during the cross-linking reaction. To increase the amount of unreacted DTC units in the system, a lower cross-linker/DTC ratio of 0.25 for poly(DTCMMA-*r*-*n*BMA) was examined (Figure S8), which results in a theoretical N %/S % of 0.25. The thin film was subsequently cross-linked upon UV light illumination, and a N %/S % ratio of 0.206 was obtained from the XPS results, which corresponds to a conversion of 0.824. These results suggest that the stoichiometry of the cross-linker to the DTC units can be utilized to tune the number of DTC and thiol groups obtained upon photocross-linking.

Multifunctional Surface Engineering. For imparting surface functionalities, the amount of the cross-linker was controlled so that the photogenerated amines are stoichiometrically less abundant than the DTC units. Three different functionalities were introduced on the cross-linked polymer thin film. First, the unreacted DTC units were functionalized with FA. Second, the thiol group generated from the ring-opening of DTC was functionalized with AB via a thiol−ene click reaction. A third functionality was introduced by making use of the comonomer of *t*BMA, by acid deprotection to liberate a carboxylic acid group which was further functionalized via EDC coupling with other amine molecules such as IA.[42] (Scheme 4) All reactions were conducted under ambient conditions, which is attractive for applications that cannot tolerate harsh reaction conditions such as high temperature. Figure 3 shows the representative XPS spectra of the photocross-linked poly(DTCMMA-*r*-*n*BMA) thin film (cross-linker/DTC unit ratio = 0.25) that underwent reaction with FA and the thiol−ene click reaction with AB. The F 1s and Br 3d peaks confirm the incorporation of the chemical groups obtained through these reactions onto the surface of the thin film. The degree of functionalization (DF) was quantitatively analyzed through the XPS spectra; the results are summarized

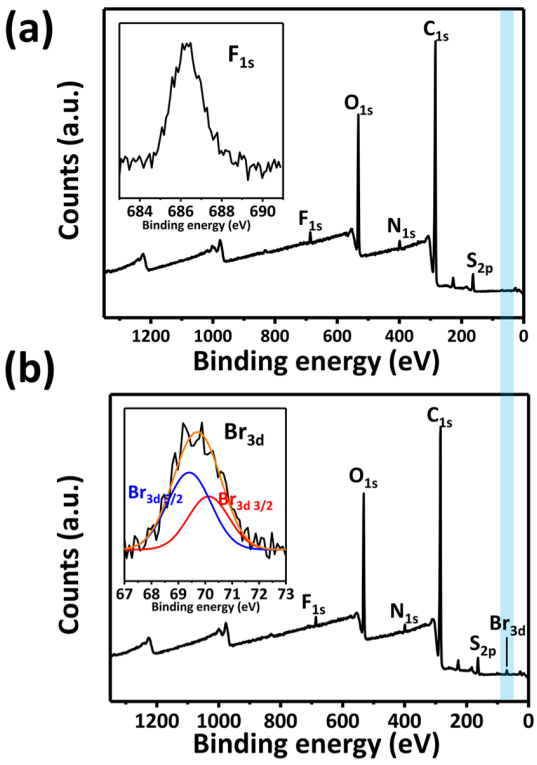

Figure 3. Representative XPS spectra of poly(DTCMMA-*r*-*n*BMA) photocross-linked thin film (DTC unit/cross-linker of 1:0.25) after functionalization via (a) DTC ring-opening with FA and (b) subsequent thiol−ene click reaction of released thiol with AB.

in Table 2 and Tables S4 and S5 (refer to the Supporting Information for more details). The DF of the first addition reaction was higher than 0.9, confirming the highly efficient reaction of the primary amines with the DTC rings. In

https://doi.org/10.1021/acsami.1c19559
ACS Appl. Mater. Interfaces 2022, 14, 3274−3283

Table 2. DF values for poly(DTCMMA-*r*-*n*BMA) and poly(DTCMMA-*r*-*t*BMA) Photocross-Linked Thin Films after Each Functionalization Step; DTC−Amine Reaction with FA, Thiol−ene Click Reaction with AB, and EDC Coupling with IA

copolymer	DTC unit/cross-linker	DF_{FA}	DF_{AB}	DF_{IA}
poly(DTCMMA-*r*-*n*BMA)	1:0.25	0.914	0.164	
poly(DTCMMA-*r*-*t*BMA)	1:0.1	0.674	0.274	0.100
poly(DTCMMA-*r*-*t*BMA)	1:0.5		0.288	
poly(DTCMMA-*r*-*t*BMA)	1:0.5[a]		0.300[a]	

[a]Before functionalization with AB, the photocross-linked thin film was treated with DTT.

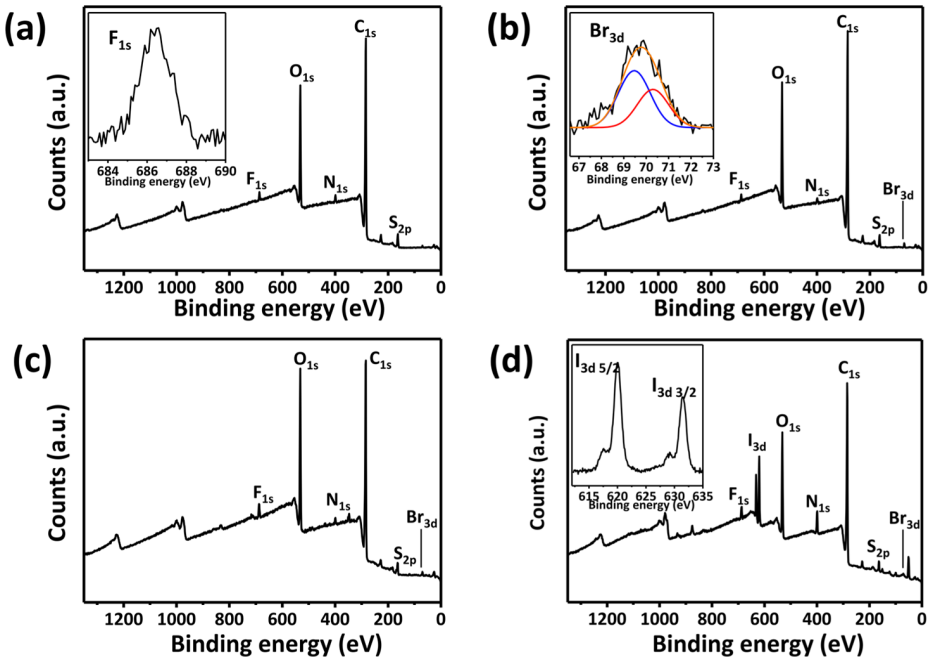

Figure 4. Representative XPS spectra of poly(DTCMMA-*r*-*t*BMA) photocross-linked thin film (DTC unit/cross-linker = 1:0.1) after functionalization via (a) DTC ring-opening reaction, (b) thiol−ene click reaction, (c) deprotection of *t*-butyl groups, and (d) EDC coupling.

contrast, the second reaction exhibited a relatively low DF value that was lower than 0.2. Typically, the light-mediated thiol−ene click reaction shows high reaction efficiencies higher than 80%,[43,44] while our results exhibited a relatively low DF in the reaction. We first hypothesized that the basic reaction conditions coming from the amine reactant[35] are responsible for the formation of disulfides, which reduce the thiol concentration and limit the reaction. This possibility was investigated with additional experiments in which the polymer film was treated with a DTT reducing agent that can break the disulfide bond before the start of the coupling reaction with AB. However, the resulting DF was found to be 0.3, which is similar to that obtained without DTT treatment (Tables 2 and S6). Hence, the low DF can likely be attributed to structural factors that reduce the reactivity of thiols present in the complex network. This hypothesis was further investigated by solution studies of the ring-opening reaction of the DTC units with FAs, which can release the thiol groups of poly(DTCMMA-*r*-*t*BMA). The efficiency of the ring opening reaction was 0.973, estimated with quantitative ^{1}H NMR analysis, confirming the high efficiency of the first reaction also in good agreement with thin film results. The material was then used for a UV light-induced click reaction with AB and DMPA. We set the concentration of DMPA to 13, 260, and 940 mol % of the released thiol following reports of the effects of the radical generator concentrations on the reaction yield.[45] The DF values of the click reaction were calculated from the ^{1}H NMR spectra (Figure S9) as 0.45, 0.37, and 0.31, respectively. These results suggest that the thiol−ene reaction is likely intrinsically limited because of the complex and bulky chemical structure of the copolymer which provides a potential limiting factor for the reaction such as the steric hindrance.

In the second set of experiments, we performed three sequential reactions on a photocross-linked thin film of poly(DTCMMA-*r*-*t*BMA) (Scheme 4 and Figure 4). The emergence of F 1s and Br 3d peaks confirm successful sequential functionalization. Upon the deprotection of *t*BMA units of the resulting surface with acid treatment (Figure S10), the subsequent EDC coupling of IA with this surface's carboxylic acid was also successful, as confirmed by the I 3d signal. After the final EDC coupling reaction on the surface, the XPS spectra showed F 1s, Br 3d, and I 3d signals, which confirm the successful incorporation of multiple functionalities. We further quantitatively analyzed the concentrations of sulfur, fluorine, bromine, and iodine (Table 2; see Table S5 and Supporting Information for details). Similar to the poly(DTCMMA-*r*-*n*BMA) thin film, the first addition and second thiol−ene reactions resulted in reasonable yields of approximately 0.7 and 0.3, respectively. The third EDC coupling reaction resulted in a DF of 0.10. These results confirm that the sequence of reactions used in this study does not significantly degrade other immobilized functionalities and that the copolymer system offers orthogonality in the surface reactions.

https://doi.org/10.1021/acsami.1c19559
ACS Appl. Mater. Interfaces 2022, 14, 3274−3283

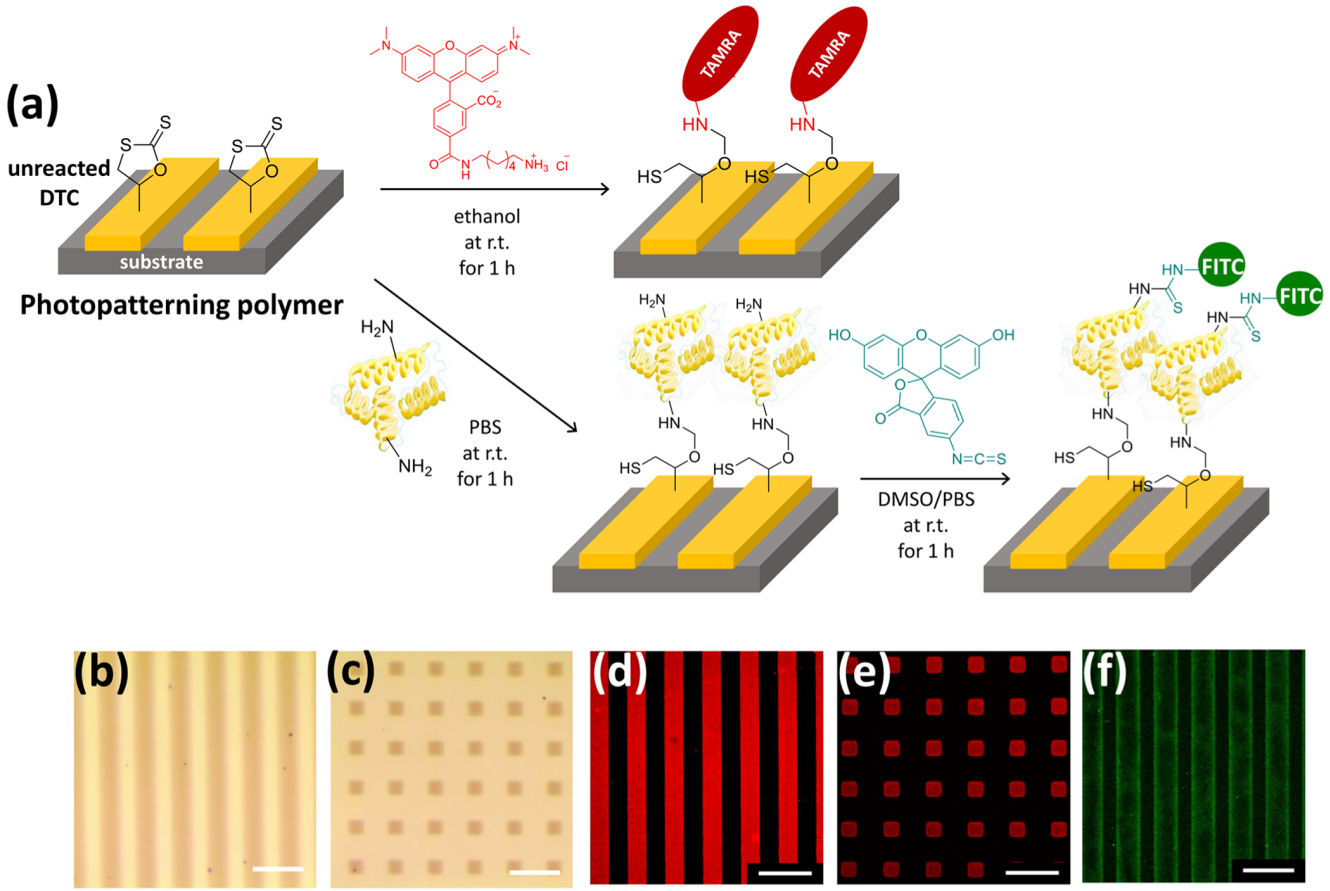

Figure 5. (a) Process for attaching various molecules on cross-linked poly(DTCMMA-*r*-*n*BMA) film. (b,c) Optical microscope images of photopatterned poly(DTCMMA-*r*-*n*BMA) (scale bar = 50 μm). CLSM images of photopatterns (d,e) functionalized with TAMRA amine and (f) functionalized with BSA and sequential labeling of FITC (scale bar = 50 μm).

Formation and Functionalization of Photopatterns. The photocross-linking mechanism for the thin film fabrication allows the formation of photopatterns. Poly(DTCMMA-*r*-*n*BMA) and poly(DTCMMA-*r*-*t*BMA) with the cross-linker were used for the fabrication of line/space (18 μm/18 μm) and periodic square (15 μm × 15 μm) patterns through a negative-tone photoresist patterning process (Figure 5b,c). The resulting width and shape of the photopatterns matched well with the standard pattern of the used photomask. In principle, the surface of the photopatterns should be functionalizable via the chemical routes described in the previous section. For example, the unreacted DTC unit present on the photopattern should be available for reaction with primary amines. We immobilized fluorophore molecules on the photopatterns to confirm this hypothesis so that the region where the reaction occurred can be readily visualized (Figure 5a). The immobilization was carried out by the reaction of red fluorophore, TAMRA amine, with the unreacted DTC group present on the line/space and periodic square patterns of the material. The creation of reactive sites at the desired locations was confirmed by CLSM (Figure 5d,e). This surface reaction was extended to the fabrication of a protein pattern, and BSA was effectively grafted using the primary amine of lysine, which reacts with the DTC groups of the surface. This reaction was confirmed by detecting the labeled FITC present on the BSA grafted on the photopattern (Figure 5f). Additional experiments with a reducing agent for disulfide cleavage further affirm that the immobilization is attributed to the reaction of amine to the DTC rather than disulfide bond formation between BSA and the surface (Figure S11). These results highlight the efficient and versatile functionalization routes that can be used to create patterns with specific surface functionalities.

■ CONCLUSIONS

We have demonstrated a photoimageable polymeric platform that can be modified with various efficient chemical reactions, resulting in surfaces with multiple chemical functionalities. The key to the fabrication of these functionalizable surfaces is synthesizing copolymers with a five-membered cyclic DTC monomer and alkyl methacrylates via RAFT polymerization. Kinetic studies show that the copolymerization follows typical pseudo-first-order kinetics and that the side reactions of the copolymerization can be suppressed at low to moderate conversion. These copolymers were successfully photocross-linked into films with only UV light illumination; the key to this efficient room temperature cross-linking is a bicomponent cross-linker that bears the *o*-nitrobenzyl group. This bicomponent cross-linkable system allowed us to create lithographically defined negative-tone patterns with controlled amounts of reactive functionalities, those being unreacted DTC, thiol released by DTC ring-opening, and carboxylic acid from the comonomer in the copolymer. These chemical groups can be used to perform effective sequential functionalization with different molecules under mild conditions. These orthogonal reactions span nucleophilic addition reaction,

https://doi.org/10.1021/acsami.1c19559
ACS Appl. Mater. Interfaces 2022, 14, 3274−3283

thiol−ene click reaction, and EDC coupling reaction. The presence of the characteristic elements (F, Br, and I) in the incorporated molecules at each step of the reaction verified by the XPS measurements allowed quantitative understanding of the extents of the surface functionalization reactions. The presented material platform was successfully adapted to incorporate structurally complex functional molecules and even biological polymer, that is, TAMRA amine fluorophore and BSA, in lithographically defined regions. The methodology described here offers a versatile means for creating coatings that can produce reactive and functional surfaces and patterns with a high degree of chemical complexity. We anticipate that these coatings will have a substantial impact on the field of biotechnology and be utilized for interfacial modification in general.

■ ASSOCIATED CONTENT

Supporting Information

The Supporting Information is available free of charge at https://pubs.acs.org/doi/10.1021/acsami.1c19559.

^{1}H NMR spectra and SEC chromatograms; characteristics of synthesized copolymers; ^{1}H and ^{13}C NMR spectra and high-resolution mass spectrum of the photocross-linker; cross-linking efficiency as a function of exposure dose; XPS spectra of photocross-linked films; quantitative XPS analyses; ^{1}H NMR spectra for solution studies of thiol−ene click reaction; and CLSM images (PDF)

■ AUTHOR INFORMATION

Corresponding Authors

Padma Gopalan − *Department of Materials Science and Engineering, University of Wisconsin, Madison, Wisconsin 53706, United States;* orcid.org/0000-0002-1955-640X; Email: pgopalan@wisc.edu

Myungwoong Kim − *Department of Chemistry and Chemical Engineering, Inha University, Incheon 22212, Republic of Korea;* orcid.org/0000-0003-0611-8694; Email: mkim233@inha.ac.kr

Authors

Sol An − *Department of Chemistry and Chemical Engineering, Inha University, Incheon 22212, Republic of Korea*

Jieun Nam − *Department of Chemistry and Chemical Engineering, Inha University, Incheon 22212, Republic of Korea*

Catherine Kanimozhi − *Department of Materials Science and Engineering, University of Wisconsin, Madison, Wisconsin 53706, United States*

Youngjoo Song − *Department of Chemistry and Chemical Engineering, Inha University, Incheon 22212, Republic of Korea*

Seungjun Kim − *Department of Chemistry and Chemical Engineering, Inha University, Incheon 22212, Republic of Korea*

Naechul Shin − *Department of Chemical Engineering and Program in Biomedical Science & Engineering, Inha University, Incheon 22212, Republic of Korea;* orcid.org/0000-0002-2630-6820

Complete contact information is available at: https://pubs.acs.org/10.1021/acsami.1c19559

Author Contributions

S.A. and J.N. contributed equally. The manuscript was written based on contributions from all authors. All authors have given approval to the final version of the manuscript.

Notes

The authors declare no competing financial interest.

■ ACKNOWLEDGMENTS

We acknowledge the support from Korea Evaluation Institute of Industrial Technology (KEIT) funded by the Ministry of Trade, Industry and Energy (MOTIE) of the Republic of Korea (project no. 20010321). P.G. acknowledges the support from the National Science Foundation (grant no. DMR-1507409). M.K. and S.K. acknowledge the partial support by the National Research Foundation of Korea (NRF) grants (2021R1A2C1093999).

■ REFERENCES

(1) An, S.; Kim, H.; Kim, M.; Kim, S. Photoinduced Modulation of Polymeric Interfacial Behavior Controlling Thin-Film Block Copolymer Wetting. *Langmuir* **2020**, *36*, 3046−3056.

(2) Jiang, Z.; Alam, M. M.; Cheng, H.-H.; Blakey, I.; Whittaker, A. K. Spatial Arrangement of Block Copolymer Nanopatterns Using a Photoactive Homopolymer Substrate. *Nanoscale Adv.* **2019**, *1*, 3078−3085.

(3) Yan, Y.; Huang, L.-B.; Zhou, Y.; Han, S.-T.; Zhou, L.; Sun, Q.; Zhuang, J.; Peng, H.; Yan, H.; Roy, V. A. L. Surface Decoration on Polymeric Gate Dielectrics for Flexible Organic Field-Effect Transistors via Hydroxylation and Subsequent Monolayer Self-Assembly. *ACS Appl. Mater. Interfaces* **2015**, *7*, 23464−23471.

(4) He, W.; Xu, W.; Peng, Q.; Liu, C.; Zhou, G.; Wu, S.; Zeng, M.; Zhang, Z.; Gao, J.; Gao, X.; Lu, X.; Liu, J.-M. Surface Modification on Solution Processable ZrO_2 High-k Dielectrics for Low Voltage Operations of Organic Thin Film Transistors. *J. Phys. Chem. C* **2016**, *120*, 9949−9957.

(5) Beier, C. W.; Cuevas, M. A.; Brutchey, R. L. Effect of Surface Modification on the Dielectric Properties of $BaTiO_3$ Nanocrystals. *Langmuir* **2010**, *26*, 5067−5071.

(6) Liu, C.; Lee, J.; Ma, J.; Elimelech, M. Antifouling Thin-Film Composite Membranes by Controlled Architecture of Zwitterionic Polymer Brush Layer. *Environ. Sci. Technol.* **2017**, *51*, 2161−2169.

(7) Jeong, W.; Kang, H.; Kim, E.; Jeong, J.; Hong, D. Surface-Initiated ARGET ATRP of Antifouling Zwitterionic Brushes Using Versatile and Uniform Initiator Film. *Langmuir* **2019**, *35*, 13268−13274.

(8) Zhao, W.; Ye, Q.; Hu, H.; Wang, X.; Zhou, F. Grafting Zwitterionic Polymer Brushes via Electrochemical Surface-Initiated Atomic-Transfer Radical Polymerization for Anti-Fouling Applications. *J. Mater. Chem. B* **2014**, *2*, 5352−5357.

(9) Inoue, Y.; Onodera, Y.; Ishihara, K. Initial Cell Adhesion onto a Phospholipid Polymer Brush Surface Modified with A Terminal Cell Adhesion Peptide. *ACS Appl. Mater. Interfaces* **2018**, *10*, 15250−15257.

(10) Li, J.; Yu, Y.; Myungwoong, K.; Li, K.; Mikhail, J.; Zhang, L.; Chang, C.-C.; Gersappe, D.; Simon, M.; Ober, C.; Rafailovich, M. Manipulation of Cell Adhesion and Dynamics Using RGD Functionalized Polymers. *J. Mater. Chem. B* **2017**, *5*, 6307−6316.

(11) Hong, S. H.; Hong, S.; Ryou, M.-H.; Choi, J. W.; Kang, S. M.; Lee, H. Sprayable Ultrafast Polydopamine Surface Modifications. *Adv. Mater. Interfaces* **2016**, *3*, 1500857.

(12) Wei, X.; Zhou, H.; Chen, F.; Wang, H.; Ji, Z.; Lin, T. High-Efficiency Low-Resistance Oil-Mist Coalescence Filtration Using Fibrous Filters with Thickness-Direction Asymmetric Wettability. *Adv. Funct. Mater.* **2019**, *29*, 1806302.

(13) Lee, H.; An, S.; Kim, S.; Jeon, B.; Paeng, K.; Kim, I. S.; Kim, M. Epoxy-Containing Copolymers: A Versatile Toolbox for Functional

Nanofiber Mats with Desired Chemical Functionalities. *Adv. Mater. Interfaces* **2018**, *5*, 1800506.
(14) Zhang, W.; Li, X.; Qu, R.; Liu, Y.; Wei, Y.; Feng, L. Janus Membrane Decorated via a Versatile Immersion-Spray Route: Controllable Stabilized Oil/Water Emulsion Separation Satisfying Industrial Emission and Purification Criteria. *J. Mater. Chem. A* **2019**, *7*, 4941−4949.
(15) Patel, P. R.; Kiser, R. C.; Lu, Y. Y.; Fong, E.; Ho, W. C.; Tirrell, D. A.; Grubbs, R. H. Synthesis and Cell Adhesive Properties of Linear and Cyclic RGD Functionalized Polynorbornene Thin Films. *Biomacromolecules* **2012**, *13*, 2546−2553.
(16) Peters, R. D.; Yang, X. M.; Kim, T. K.; Sohn, B. H.; Nealey, P. F. Using Self-Assembled Monolayers Exposed to X-rays to Control The Wetting Behavior of Thin Films of Diblock Copolymers. *Langmuir* **2000**, *16*, 4625−4631.
(17) Sun, Y.-S.; Wang, C.-T.; Liou, J.-Y. Tuning Polymer-Surface Chemistries and Interfacial Interactions with UV Irradiated Polystyrene Chains to Control Domain Orientations in Thin Films of PS-*b*-PMMA. *Soft Matter* **2016**, *12*, 2923−2931.
(18) Sprick, R. S.; Cheetham, K. J.; Bai, Y.; Alves Fernandes, J.; Barnes, M.; Bradley, J. W.; Cooper, A. I. Polymer Photocatalysts with Plasma-Enhanced Activity. *J. Mater. Chem. A* **2020**, *8*, 7125−7129.
(19) Yang, W.-C.; Wu, S.-H.; Chen, Y.-F.; Nelson, A.; Wu, C.-M.; Sun, Y.-S. Effects of The Density of Chemical Cross-Links and Physical Entanglements of Ultraviolet-Irradiated Polystyrene Chains on Domain Orientation and Spatial Order of Polystyrene-*block*-Poly (methyl methacrylate) Nano-Domains. *Langmuir* **2019**, *35*, 14017−14030.
(20) Welch, M. E.; Doublet, T.; Bernard, C.; Malliaras, G. G.; Ober, C. K. A Glucose Sensor via Stable Immobilization of The GOx Enzyme on an Organic Transistor Using A Polymer Brush. *J. Polym. Sci., Part A: Polym. Chem.* **2015**, *53*, 372−377.
(21) Carroll, G. T.; Sojka, M. E.; Lei, X.; Turro, N. J.; Koberstein, J. T. Photoactive Additives for Cross-Linking Polymer Films: Inhibition of Dewetting in Thin Polymer Films. *Langmuir* **2006**, *22*, 7748−7754.
(22) Spruell, J. M.; Wolffs, M.; Leibfarth, F. A.; Stahl, B. C.; Heo, J.; Connal, L. A.; Hu, J.; Hawker, C. J. Reactive, Multifunctional Polymer Films through Thermal Cross-Linking of Orthogonal Click Groups. *J. Am. Chem. Soc.* **2011**, *133*, 16698−16706.
(23) Hong, J.; Choi, S.; Jwa, D. G.; Kim, M.; Kang, S. M. Mussel-Inspired, One-Step Thiol Functionalization of Solid Surfaces. *Langmuir* **2020**, *36*, 1608−1614.
(24) Wang, R.; Chen, W.; Meng, F.; Cheng, R.; Deng, C.; Feijen, J.; Zhong, Z. Unprecedented Access to Functional Biodegradable Polymers and Coatings. *Macromolecules* **2011**, *44*, 6009−6016.
(25) Wang, X.; Liu, G.; Hu, J.; Zhang, G.; Liu, S. Concurrent Block Copolymer Polymersome Stabilization and Bilayer Permeabilization by Stimuli-Regulated "Traceless" Crosslinking. *Angew. Chem., Int. Ed.* **2014**, *53*, 3138−3142.
(26) Wang, X.; Hu, J.; Liu, G.; Tian, J.; Wang, H.; Gong, M.; Liu, S. Reversibly Switching Bilayer Permeability and Release Modules of Photochromic Polymersomes Stabilized by Cooperative Noncovalent Interactions. *J. Am. Chem. Soc.* **2015**, *137*, 15262−15275.
(27) Yao, C.; Li, Y.; Wang, Z.; Song, C.; Hu, X.; Liu, S. Cytosolic NQO1 Enzyme-Activated Near-Infrared Fluorescence Imaging and Photodynamic Therapy with Polymeric Vesicles. *ACS Nano* **2020**, *14*, 1919−1935.
(28) Liu, X.; Li, M.; Han, T.; Cao, B.; Qiu, Z.; Li, Y.; Li, Q.; Hu, Y.; Liu, Z.; Lam, J. W. Y.; Hu, X.; Tang, B. Z. In Situ Generation of Azonia-Containing Polyelectrolytes for Luminescent Photopatterning and Superbug Killing. *J. Am. Chem. Soc.* **2019**, *141*, 11259−11268.
(29) Hu, X.; Zhao, X.; He, B.; Zhao, Z.; Zheng, Z.; Zhang, P.; Shi, X.; Kwok, R. T. K.; Lam, J. W. Y.; Qin, A.; Tang, B. Z. A Simple Approach to Bioconjugation at Diverse Levels: Metal-Free Click Reactions of Activated Alkynes with Native Groups of Biotargets without Prefunctionalization. *Research* **2018**, *2018*, 3152870.
(30) Krutty, J. D.; Schmitt, S. K.; Gopalan, P.; Murphy, W. L. Surface Functionalization and Dynamics of Polymeric Cell Culture Substrates. *Curr. Opin. Biotechnol.* **2016**, *40*, 164−169.
(31) Schmitt, S. K.; Murphy, W. L.; Gopalan, P. Crosslinked PEG Mats for Peptide Immobilization and Stem Cell Adhesion. *J. Mater. Chem. B* **2013**, *1*, 1349−1360.
(32) Kim, G.; An, S.; Hyeong, S.-K.; Lee, S.-K.; Kim, M.; Shin, N. Perovskite Pattern Formation by Chemical Vapor Deposition Using Photolithographically Defined Templates. *Chem. Mater.* **2019**, *31*, 8212−8221.
(33) Vanbiervliet, E.; Fouquay, S.; Michaud, G.; Simon, F.; Carpentier, J.-F.; Guillaume, S. M. From Epoxide to Cyclodithiocarbonate Telechelic Polycyclooctene through Chain-Transfer Ring-Opening Metathesis Polymerization (ROMP): Precursors to Non-Isocyanate Polyurethanes (NIPUs). *Macromolecules* **2017**, *50*, 69−82.
(34) Kihara, N.; Nakawaki, Y.; Endo, T. Preparation of 1, 3-Oxathiolane-2-thiones by the Reaction of Oxirane and Carbon Disulfide. *J. Org. Chem.* **1995**, *60*, 473−475.
(35) Hirata, M.; Watanabe, T.; Ochiai, B.; Endo, T. Synthesis of Graft Terpolymers by Addition Reaction of Amino-Terminated Polyether to Poly(methacrylate)s Bearing Five-Membered Cyclic Dithiocarbonate Moieties and Application of the Graft Terpolymers as Modifiers for Wool. *J. Polym. Sci., Part A: Polym. Chem.* **2012**, *50*, 3259−3268.
(36) Konkolewicz, D.; Hawkett, B. S.; Gray-Weale, A.; Perrier, S. RAFT Polymerization Kinetics: Combination of Apparently Conflicting Models. *Macromolecules* **2008**, *41*, 6400−6412.
(37) Miyata, T.; Matsumoto, K.; Endo, T.; Yonemori, S.; Watanabe, S. Synthesis and Radical Polymerization of Styrene-Based Monomer Having a Five-Membered Cyclic Dithiocarbonate Structure. *J. Polym. Sci., Part A: Polym. Chem.* **2013**, *51*, 1398−1404.
(38) Bernkop-Schnürch, A.; Scholler, S.; Biebel, R. G. Development of Controlled Drug Release Systems Based on Thiolated Polymers. *J. Controlled Release* **2000**, *66*, 39−48.
(39) Goethals, F.; Frank, D.; Du Prez, F. Protected Thiol Strategies in Macromolecular Design. *Prog. Polym. Sci.* **2017**, *64*, 76−113.
(40) Umar, M.; Son, D.; Arif, S.; Kim, M.; Kim, S. Multistimuli-Responsive Optical Hydrogel Nanomembranes to Construct Planar Color Display Boards for Detecting Local Environmental Changes. *ACS Appl. Mater. Interfaces* **2020**, *12*, 55231−55242.
(41) Bochet, C. G. Photolabile Protecting Groups and Linkers. *J. Chem. Soc., Perkin Trans. 1* **2002**, 125−142.
(42) Fischer, M. J. E. Amine Coupling through EDC/NHS: A Practical Approach. *Surface Plasmon Resonance*; Springer, 2010; pp 55−73.
(43) Tucker-Schwartz, A. K.; Farrell, R. A.; Garrell, R. L. Thiol−Ene Click Reaction as a General Route to Functional Trialkoxysilanes for Surface Coating Applications. *J. Am. Chem. Soc.* **2011**, *133*, 11026−11029.
(44) Love, D. M.; Kim, K.; Goodrich, J. T.; Fairbanks, B. D.; Worrell, B. T.; Stoykovich, M. P.; Musgrave, C. B.; Bowman, C. N. Amine Induced Retardation of the Radical-Mediated Thiol−Ene Reaction via the Formation of Metastable Disulfide Radical Anions. *J. Org. Chem.* **2018**, *83*, 2912−2919.
(45) Derboven, P.; D'hooge, D. R.; Stamenovic, M. M.; Espeel, P.; Marin, G. B.; Du Prez, F. E.; Reyniers, M.-F. Kinetic Modeling of Radical Thiol−Ene Chemistry for Macromolecular Design: Importance of Side Reactions and Diffusional Limitations. *Macromolecules* **2013**, *46*, 1732−1742.

https://doi.org/10.1021/acsami.1c19559
ACS Appl. Mater. Interfaces 2022, 14, 3274−3283